

Large-eddy simulations in dune-dynamics research

Ugo Piomelli ⁽¹⁾ and Mohammad Omidyeganeh ⁽¹⁾

1. Department of Mechanical and Materials Engineering, Queen's University, Kingston (ON), Canada - ugo@me.queensu.ca, omidyeganeh@me.queensu.ca

Abstract

We discuss the recent use of large-eddy simulations (LES) for the analysis of the flow over dunes. In large-eddy simulations the governing equations of fluid motion are solved on a grid sufficiently fine to resolve the largest eddies, while the effect of the smallest ones is modelled. Examples are shown to demonstrate how this technique can be used to complement experiments, by exploiting its ability to calculate full-field information, and to highlight the temporal development of the flow. The main challenges slowing a more widespread application of this method are discussed.

1. INTRODUCTION

The study of environmental and geophysical flows presents considerable challenges. Geometrical complexities, stratification, two-phase flows are often present. Field experiments are extremely difficult, due to the often adverse conditions, and to the difficulty in obtaining accurate full-field measurements, especially near solid boundaries, and to the lack of control over the boundary conditions. Laboratory-scale studies can overcome some of these issues, but are still limited: in addition to the fact that a reduced Reynolds number must be used, present experimental techniques force the researcher to compromise between conflicting requirements: the needs for time-resolved measurements, for all components of the velocity, and for full-field information are difficult to reconcile. Furthermore, simultaneous measurements of velocity and scalars cannot always be obtained, and some quantities (vorticity, pressure, for instance) are difficult to measure.

Numerical models have recently been applied with increased frequency, due to the decreasing cost of computational power. Early simulations solved the Reynolds-Averaged Navier-Stokes (RANS) equations (Mendoza & Shen, 1990; Yoon and Patel,

1996). In RANS solutions the contribution of all the turbulent motions (eddies) is parameterized; in complex flows out of fluid-dynamical equilibrium these models may be inaccurate; moreover, they cannot account for the unsteady nature of turbulence. In many cases large coherent motions ("macro-turbulence", Best 2005) are responsible for much of the momentum, energy and scalar transport. In this conditions, more advanced models are required to give accurate predictions of the flow, and help understand the turbulence physics underlying the transport processes.

One of these methods is the large-eddy simulation (LES). In LES the contribution of the large, energy-carrying structures to momentum and energy transfer is computed exactly, and only the effect of the smallest scales of turbulence is modelled. Since the small scales tend to be more homogeneous and universal, and less affected by the boundary conditions than the large ones, there is hope that their models can be simpler, and require fewer adjustments when applied to different flows, than similar models for the RANS equations.

LES provide a three-dimensional, time dependent solution of the Navier-Stokes equations. Among the objectives of LES are to provide data for low-

er-level turbulence models at moderate to high Reynolds numbers, and to study complex physics in realistic configurations.

While LES has a long history in the environmental sciences (in particular, meteorology), and in mechanical and aerospace engineering, its use for the study of dune dynamics is more recent. The first LES of this type was carried out by Yue and co-workers (Yue *et al.*, 2005). They modelled the flow over two-dimensional dunes for two depths. The results showed that the interaction of the free surface and the flow structures is significantly affected by the flow depth. The same authors (Yue *et al.*, 2006) subsequently performed LES in nearly the same configuration, and visualized periodically flapping spanwise rollers in the recirculation zone. Stoesser *et al.* (2008) showed rollers at the crest that expanded to the size of the dune height as they were convected towards the reattachment point, and conjectured that the boils on the surface were originally hairpin eddies generated in the reattachment region as a result of secondary instabilities of rollers that are elongated in the streamwise direction and tilted upward. However, the instantaneous visualizations of velocity fluctuations do not show a strong upwelling at the surface, but rather a structure more similar to the smaller, weaker boils that occur at the surface of open-channel flows over flat surfaces.

Grigoriadis *et al.* (2009) studied two cases with Reynolds numbers (based on average flow depth and mean bulk velocity) equal to 17,500 and 93,500. They examined the turbulent eddies in more detail than previous investigators. Their results, however, differ somewhat from previous experimental and numerical observations: in their simulations the horseshoe structures do not reach the surface. They, however, observed kolk vortices generated by the interaction between streamwise vortices that reach the dune crest from upstream and rollers generated at the crest. Kolk vortices were found to last for long times, and were the most significant structure observed at the surface in their simulations.

Recently, we have applied LES to the study of two and three-dimensional dunes, at laboratory scale (Omidyeganeh & Piomelli, 2011, 2013). Our studies have focused on the relation between the largest coherent eddies, which may be generated in the separated or by the three-dimensionality of the bedform, to the mean and instantaneous flow. The

type of understanding that can be obtained through a quantitative and qualitative analysis of the data obtained from such simulations will be discussed in Section 3.

In the following, first, a typical LES model will be described. Then, some representative results will be shown to illustrate the potential of this method. Finally, the potential and shortcomings of LES, *vis-à-vis* its application to dune dynamics, will be discussed.

2. METHODOLOGY

2.1 Governing equations

Large-eddy simulations (LES) are based on the assumption that small-scale turbulent eddies are more isotropic than the large ones, and are responsible mostly for energy dissipation in the mean. Modelling the small scales, while resolving the larger eddies, may be very beneficial: first, since most of the momentum transport is due to the large eddies, model inaccuracies are less critical; secondly, the modelling of the unresolved scales is easier, since they tend to be more homogeneous and isotropic than the large ones, which depend on the boundary conditions.

Thus, LES is based on the use of a filtering operation: a filtered (or resolved, or large-scale) variable, denoted by an overbar, is defined as

$$\bar{f}(\mathbf{x}) = \int_D f(\mathbf{x}') G(\mathbf{x}, \mathbf{x}') d\mathbf{x}' \quad (1)$$

where D is the entire domain and G is the *filter* function (Leonard 1974).

The filter function determines the size and structure of the small scales. The size of the smallest eddies that are resolved in LES is related to the length-scale of the smoothing operator, the “filter width”, $\bar{\Delta}$. The grid size, h , should be sufficiently fine to allow eddies of size $\bar{\Delta}$ to be represented accurately.

If the operation (1) is applied to the governing equations, one obtains the filtered equations of motion, which are solved in large-eddy simulations. For an incompressible flow of a Newtonian fluid, they take the following form:

$$\frac{\partial \bar{u}_i}{\partial x_i} = 0 \quad (2)$$

$$\frac{\partial \bar{u}_i}{\partial t} + \frac{\partial}{\partial x_j} (\bar{u}_i \bar{u}_j) = -\frac{1}{\rho} \frac{\partial \bar{p}}{\partial x_i} - \frac{\partial \tau_{ij}}{\partial x_j} + \nu \nabla^2 \bar{u}_i \quad (3)$$

$$\frac{\partial \bar{c}}{\partial t} + \frac{\partial}{\partial x_j} (\bar{c} u_j) = - \frac{\partial Q_j}{\partial x_j} + \kappa \nabla^2 \bar{c} \quad (4)$$

where c is an arbitrary transported scalar, ρ is the fluid density, p its pressure, ν and κ are, respectively, the kinematic viscosity and the molecular diffusivity of c , and τ_{ij} and Q_j are the subgrid-scale (SGS) stresses and scalar flux, defined as

$$\tau_{ij} = \bar{u_i u_j} - \bar{u_i} \bar{u_j}; \quad Q_j = \bar{u_j c} - \bar{u_j} \bar{c} \quad (5)$$

These terms must be parameterized; eddy-viscosity and diffusivity models are generally considered adequate (Piomelli 1999, Meneveau & Katz 2000).

2.2 Numerical approach

Most of the applications of LES to dune dynamics employ structured, finite difference or finite-volume codes, either using body-fitted or Cartesian grids. Our numerical method, in particular, is a curvilinear finite-volume code. Both convective and diffusive fluxes are approximated by second-order central differences. A second-order-accurate semi-implicit fractional-step procedure (Kim & Moin 1985) is used for the temporal discretization. The Crank-Nicolson scheme is used for the wall-normal diffusive terms, and the Adams-Bashforth scheme for all the other terms. The pressure is obtained from the solution of a Poisson equation, which will be discussed later. The code is parallelized using the Message-Passing Interface and the domain-decomposition technique, and has been extensively tested for turbulent flows (Silva Lopes & Palma 2002; Silva Lopes et al. 2006; Radhakrishnan et al. 2006, 2008; Omidyeganeh & Piomelli 2011).

2.3 Turbulence models

Most subgrid scale models in use presently are eddy-viscosity models of the form

$$\tau_{ij} - \delta_{ij} \tau_{kk} / 3 = -2\nu_T \bar{S}_{ij} = -2C \bar{\Delta}^2 |\bar{S}| \bar{S}_{ij}. \quad (6)$$

Here

$$\bar{S}_{ij} = (\partial \bar{u_i} / \partial x_j + \partial \bar{u_j} / \partial x_i) / 2 \quad (7)$$

is the resolved strain-rate tensor, $|\bar{S}|$ is its magnitude, ν_T is the eddy viscosity, and C is a coefficient

that, in the present simulations, is calculated using the Lagrangian-dynamic eddy-viscosity model (Meneveau *et al.*, 1996). This technique allows the eddy viscosity to respond to the local state of the flow, and adapt to fluid-dynamical non-equilibrium better than fixed-constant models.

3. CASE STUDIES

In this Section we show two examples of recent results obtained by our group, to demonstrate how numerical simulations can complement experimental studies, both at the field and at the laboratory scale to answer outstanding questions in dune dynamics.

3.1 The origin of boils

One feature of the flow over dunes that has attracted significant attention is the variety of very large (with size comparable to the river depth) coherent structures that are observed. Several researchers have discussed these structures, and their role in the transport of mass and momentum. Best (2005) observed boils (upwelling motions at the water surface, that usually occur when a horizontally oriented vortex attaches to the surface) in a high Reynolds-number flow over dunes in the laboratory and in the Jamuna River, Bangladesh, and proposed a schematic model for the interaction of coherent structures with the flow surface that results in boils. Discussion on the generation of large vortex loops that cause the strong upwelling at the surface is still inconclusive. Müller and Gyr (1986) proposed a mixing-layer analogy in which separated spanwise vortices at the crest undergo three-dimensional instabilities, which eventually cause hairpin-like vortices associated with low-speed fluid that rises up to the surface and generates boils. Nezu & Nakagawa (1993) identified vortices in the separated-flow region that move towards the reattachment point; they conjecture that kolk-boil vortices are formed due to oscillations of the reattachment line.

To determine which of the above conjectures is the correct one, we performed numerical simulations of the flow over a two-dimensional dune, at laboratory scale (Omidyeganeh & Piomelli 2011). The simulation used $416 \times 128 \times 384$ grid points to discretize a domain of dimensions $20h \times 4h \times 16h$ (where h is the dune height) at $Re=18,900$. The results of the model were validated by comparison against experimental data (Balachandar *et al.*

2003).

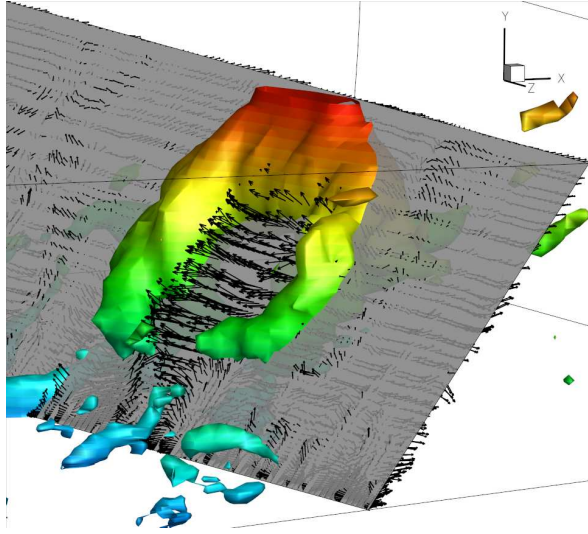


Figure 1. Visualization of the flow near a large horseshoe structure (visualized through isosurfaces of p' coloured by the vertical coordinate) when it touches the surface. The vectors show the upwash between the vortex legs that results in the appearance of a boil on the surface.

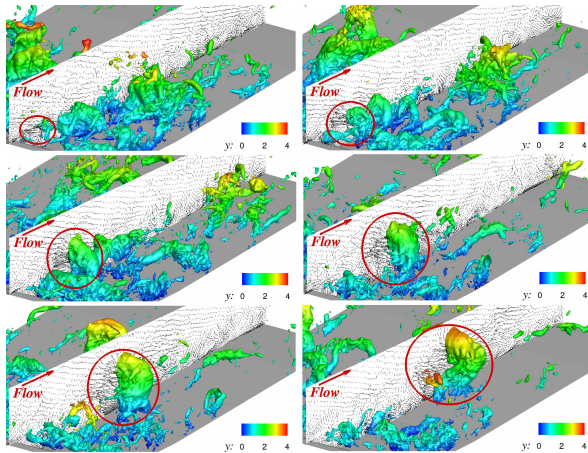


Figure 2. Evolution of a large horseshoe structure, visualized through isosurfaces of p' coloured by the vertical coordinate; the time interval between snapshots is $3h/U_b$; vectors of velocity fluctuations are shown on a vertical plane at $z = 10.7h$ for every 5 grid points.

The availability of three-dimensional velocity fields makes it possible to use advanced flow-visualization techniques. Moreover, since several snapshots of the flow, closely spaced in time, are available, one can observe a feature of interest, and

then march forward in time to study its development, but also backwards to investigate its origins. Taking advantage of these features of the numerical model, and coupling the (qualitative) flow visualization with a quantitative analysis, allows us to obtain in-depth understanding that would be difficult to achieve using experimental techniques, especially at field scale.

Figure 1, for instance, shows the flow field associated with a horseshoe vortex that reaches the water surface. The vortex is visualized through isosurfaces of the pressure fluctuations, negative values of which highlight the core of large scale vortices. We observe, first, that the scale of the vortex is comparable to the depth, consistent with many experimental observations. Second, that the vortex induces a very strong upwash between its legs, which causes with the vertical velocity, high pressure and diverging streamlines associated with a boil.

The temporal development of a horseshoe vortex of this type is illustrated in Figure 2, which shows how a spanwise vortex generated at the separation point undergoes a 3D instability, and moves towards the surface while, at the same time, becoming more and more 3D and assuming its characteristic horseshoe shape.

A more quantitative illustration of this development is given in Figure 3, in which we show the probability of the occurrence of the vortices that cause the boils. A very clear high-probability region extends from the separation point at the dune top, towards the free surface over the stoss side. Spectra measured along this path show a distinct peak that corresponds to the shedding frequency; this signature can be observed even at the surface, in regions where boils prevalently occur. The reattachment region, or the boundary layer on the stoss side, by contrast, do not show this signature.

3.2 Dune three-dimensionality

A similar approach was taken by Omidyeganeh & Piomelli (2013) to study the effect of crest three-dimensionality on the flow field. A sinusoidal deformation was imposed on the crestline, and cases with varying amplitude and wavelength were studied. One case in which the lobes and saddles were staggered was also considered.

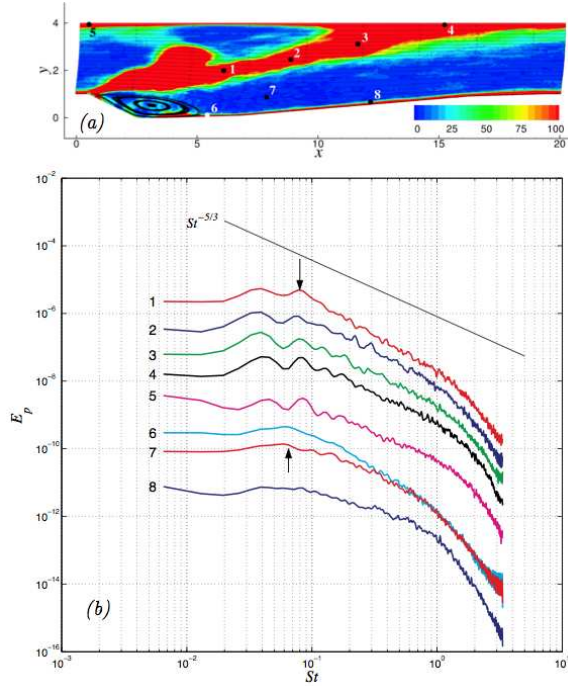


Figure 2. (a) Contours of the number of occurrence of the event $p' < -5prms$; (b) pressure spectra at the points marked in (a); each curve is shifted downward by a factor of 10 for clarity.

Allen (1968) studied near bed streamlines of a series of sinusoidal crestline dunes and obtained some insight of the developed secondary flow across the channel. The induced streamwise vortices with a size of the flow depth are measured by Maddux and co-workers (Maddux *et al.* 2003a, 2003b) for a staggered crestline configuration. The characteristics of these vortices have been related to the characteristics of the sinusoidal crestline by Venditti (2007) for aligned crestline configurations. Our simulations provide features of the secondary flows, their impact on the bed shear stress distribution, characteristics of the separation and reattachment regions, and sensitivity of turbulence statistics to the geometrical parameters of the crestlines.

Figure 4 shows contours of the streamwise component of the wall stress, for three selected cases. The dashed white lines highlight the $\tau_{w,x} = 0$ contour. First, we note that longitudinal regions of low wall stress can be observed in all cases. In the first case (Figures 4(a)) they are aligned with the lobe,

and are due to pairs of streamwise vortices, which advect low-speed fluid close to the bed towards the lobe and high-speed fluid from the outer flow towards the wall, thereby decreasing τ_w at the lobe and increasing it at the saddle. These vortices can be observed in Figure 5(a). In Case 9 (Figure 4(b)), in which the wavelength of the crest is short, streaks are due to a streamline convergence caused by the bottom topography, whereas in Case 10 (long wavelength and staggered dunes), two pair of vortices are present, one generated at the lobe, the other at the lobe of the upstream dune.

Case 9 has the lowest crestline wavelength, and different mean-flow characteristics. The typical secondary flow with large streamwise vortices between the lobe and the saddle, observed in the other cases, is not observed here (Figure 5(b)). In the channel interior, the spanwise velocity is negligible compared to the vertical one, and the flow characteristics are similar to the 2D dunes (Omidyeganeh & Piomelli 2011), as fluid moves downward in the first half of the channel and upward in the second half. Nezu & Nakagawa (1993) pointed out that large secondary currents occur when the wavelength of the bed deformations in the spanwise direction is more than twice the flow depth; in Case 9 the wavelength is equal to the maximum flow depth ($\lambda = 4h$), and large-scale streamwise vortices are not observed. Although the streamwise vorticity in the interior of the channel is small, due to the waviness of the bed in the spanwise direction, the spanwise pressure gradient becomes significant, driving high-momentum fluid toward the lobe, causing high-pressure zone at the lobe and low wall-shear stress stripes along the saddle plane in Figure 4(b).

In Case 10, because of the staggered lobes and saddles, the flow develops quite differently (Figures 4(c) and 5(c)). First, as was also observed experimentally (Figure 6 in Maddux *et al.* (2003a)), the flow is faster over the node plane. After the reattachment on the stoss side (e.g., in the vertical planes in Figure 5(c)), two strong vorticity contours with opposite signs are observed near the lobe. These vortices decay as they travel over the saddle plane of the following dune, but can still be observed in the vertical plane in Figure 5(c), and in the wall-stress contours in Figure 4(c).

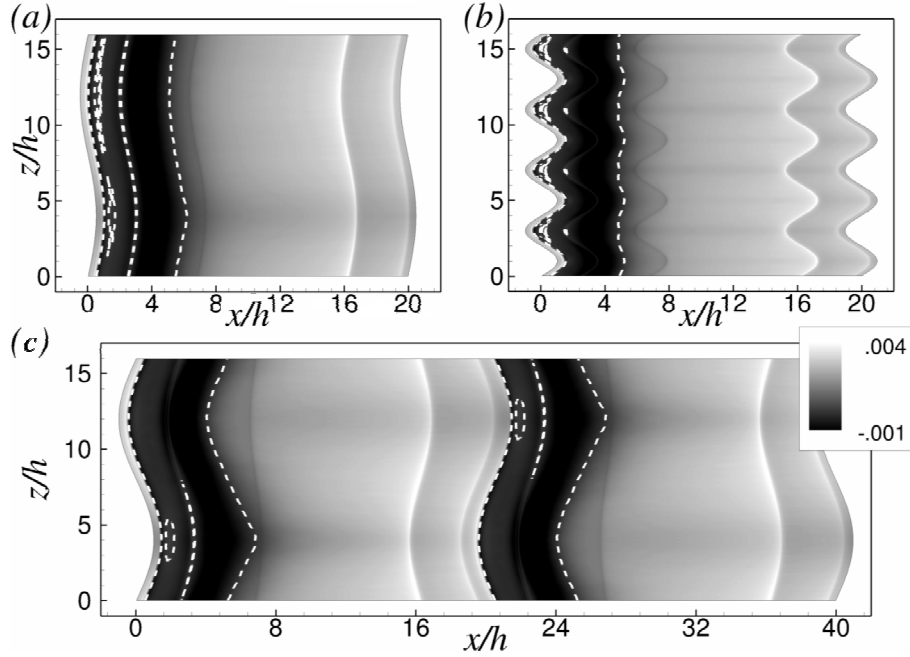


Figure 4. Contours of the streamwise component of the wall stress, $\tau_{w,x} / \rho U_b^2$. The dashed white lines highlight the $\tau_{w,x} = 0$ contour. (a) Case 1 (long crest wavelength) (b) Case 9 (short crest wavelength); (c) Case 10 (long crest wavelength, staggered dunes).

4. CHALLENGES AND ACHIEVEMENTS

Numerical simulations will not replace experiments, either at the laboratory scale, or at the field scale, in the near future. They can, however, complement them, and help researchers gain a stronger foothold on the very complex and challenging problem of turbulence in environmental flows.

Numerical models present several useful characteristics: they allow very careful definition of the boundary conditions; they yield three-dimensional and time-dependent fields, from which quantities that are hard to measure may be extracted (pressure, vorticity, higher-order moments); they allow the researcher to “travel back in time”, by isolating a flow feature of interest, and examining the flow at previous times to determine its origin; finally, in wall-resolved calculations, the flow field extends all the way to the wall. In the previous Section, through two examples of recent calculations, we have tried to show how these potential advantages can be beneficial, and allow to answer conclusively questions that had been raised by experimentalists, but could not be answered completely

based on the data available in field or laboratory studies. Additional features that can be easily added to the model are more complex geometries (either through body-fitted grids or using Immersed-Boundary Methods (Mittal & Iaccarino, 2005), the transport of pollutants or nutrients, or roughness (which, again, can be included through immersed-boundary methods).

Several challenges still limit the application of numerical models. First is the computational cost. Wall-resolved LES of the type described here are expensive, since the equations of motion need to be integrated for long times to accumulate the sample required for convergence of the statistics. In the present case, this resulted in approximately 6,000 CPU hours, or four weeks of continuous running on 64 processors. Increasing the Reynolds number to field scale is, at the present time, unfeasible, as the number of points required to resolve the flow scales like $Re^{13/7}$ (Choi & Moin 2012). The use of wall-models may allow such extension, but the additional modelling required may make the prediction of flow features that are driven by near-wall dynamics (some of the secondary flows described above, for instance) inaccurate.

Another important addition to the model is the inclusion of the motion of sand, which could help predict dune motion, or scouring. Models that include the motion of solid particles are in widespread use in engineering. Methods in which the motion of the particles (and their effect on the flow field) is simulated using a Lagrangian viewpoint are very successful for heavy particles with low concentration (solid particles in gases, for instance). In the case of flow over dunes, the density ratio between sand and water is not large, and the concentration of particles may be very large near the bottom; Eulerian approaches in which the suspended sediment is modelled as a transported scalar may be more successful. A model for the particle lift up from the wall that is accurate locally and instantaneously (and not only capable of predicting average quantities) is crucial to the development of this type of technique.

In summary, the application of LES to dune flows is quite new, but has already shown potential. A wise use of numerical simulations will, at this time, focus on fairly simple geometries, to maximize the accuracy of the model, and try to address questions that cannot be resolved adequately by present experimental techniques. As computational power continues to increase, however, there is reason to believe that predictive calculations in realistic geometries may become more and more common.

5. ACKNOWLEDGMENT

This research was supported by the Natural Sciences and Engineering Research Council (NSERC) under the Discovery Grant program. The authors thank the High Performance Computing Virtual Laboratory (HPCVL), Queen's University site, for the computational support. MO acknowledges the partial support of NSERC under the Alexander Graham Bell Canada NSERC Scholarship Program. UP also acknowledges the support of the Canada Research Chairs Program.

6. REFERENCES

- Allen, J. R. L. (1968). *Current ripples: their relation to patterns of water and sediment motion*. North-Holland Pub. Co.
- Best, J. (2005). The fluid dynamics of river dunes: A review and some future research directions. *J. Geophys. Res.*, 119(F04S02):1–21.
- Choi, H. and Moin, P. (2012). Grid-point requirements for large eddy simulation: Chapman's estimates revisited. *Phys. Fluids*, 011702.
- Grigoriadis, D. G. E., Balaras, E., and Dimas, A. A. (2009). Large-eddy simulations of unidirectional water flow over dunes. *J. Geophys. Res.*, 114.
- Kadota, A. and Nezu, I. (1999). Three-dimensional structure of space-time correlation on coherent vortices generated behind dune crests. *J. Hydr. Res.*, 37(1):59–80.
- Kim, J. and Moin, P. (1985). Application of a fractional step method to incompressible Navier-Stokes equations. *J. Comput. Phys.*, 59:308–323.
- Leonard, A. (1974). Energy cascade in large-eddy simulations of turbulent fluid flows. *Adv. Geophys.*, 18A:237–248.
- Maddux, T. B., McLean, S. R., and Nelson, J. M. (2003a). Turbulent flow over three-dimensional dunes: 2. Fluid and bed stresses. *J. Geophys. Res.*, 108-F1(6010):11–1–17.
- Maddux, T. B., Nelson, J. M., and McLean, S. R. (2003b). Turbulent flow over three-dimensional dunes: 1. Free surface and flow response. *J. Geophys. Res.*, 108-F1(6009):10–1–20.
- Mendoza, C. and Shen, H. W. (1990). Investigation of turbulent flow over dunes. *J. Hydr. Engng*, 116:459–477.
- Meneveau, C., Lund, T. S., and Cabot, W. H. (1996). A Lagrangian dynamic subgrid-scale model of turbulence. *J. Fluid Mech.*, 319:353–385.
- Meneveau, C. and Katz, J. (2000). Scale-invariance and turbulence models for large-eddy simulations. *Annu. Rev. Fluid Mech.*, 32:1–32.
- Mittal, R. and Iaccarino, G. (2005). Immersed boundary methods. *Annu. Rev. Fluid Mech.*, 37(1):239–261.
- Müller, A. and Gyr, A. (1986). On the vortex formation in the mixing layer behind dunes. *J. Hydr. Res.*, 24:359–375.
- Nezu, I. and Nakagawa, H. (1993). *Turbulence in Open-Channel Flows*. Balkema.
- Omidyeganeh, M. and Piomelli, U. (2011). Large-eddy simulation of two-dimensional dunes in a steady, unidirectional flow. *J. Turbul.*, 12(N42):1–31.
- Omidyeganeh, M. and Piomelli, U. (2013). Large-eddy simulation of three-dimensional dunes in a steady, unidirectional flow. Part 1: Turbulence statistics. *J. Fluid Mech.*
- Piomelli, U. (1999). Large-eddy simulation: achievements and challenges. *Prog. Aerosp. Sci.*, 35:335–362.
- Radhakrishnan, S., Piomelli, U., Keating, A., and Silva Lopes, A. (2006). Reynolds-averaged and large-eddy simulations of turbulent non-equilibrium flows. *J. Turbul.*, 7(63):1–30.

- Silva Lopes, A. and Palma, J. M. L. M. (2002). Simulations of isotropic turbulence using a non-orthogonal grid system. *J. Comput. Phys.*, 175(2):713–738.
- Silva Lopes, A., Piomelli, U., and Palma, J. M. L. M. (2006). Large-eddy simulation of the flow in an S-duct. *J. Turbul.*, 7(11):1–24.
- Stoesser, T., Braun, C., García-Villalba, M., and Rodi, W. (2008). Turbulence structures in flow over two-dimensional dunes. *J. Hydr. Engng*, 134(1):42–55.
- Venditti, J. G. (2007). Turbulent flow and drag over fixed two- and three-dimensional dunes. *J. Geophys. Res.*, 112(F04008):1–21.
- Yoon, J. Y. and Patel, V. C. (1996). Numerical model of turbulent flow over sand dune. *J. Hydr. Engng*, 122:10–18.
- Yue, W., Lin, C., and Patel, V. (2005). Large eddy simulation of turbulent open-channel flow with free surface simulated by level set method. *Phys. Fluids*, 17:025108.
- Yue, W., Lin, C.-L., and Patel, V. C. (2006). Large-eddy simulation of turbulent flow over a fixed two-dimensional dune. *J. Hydr. Engng*, 132(7):643–651.

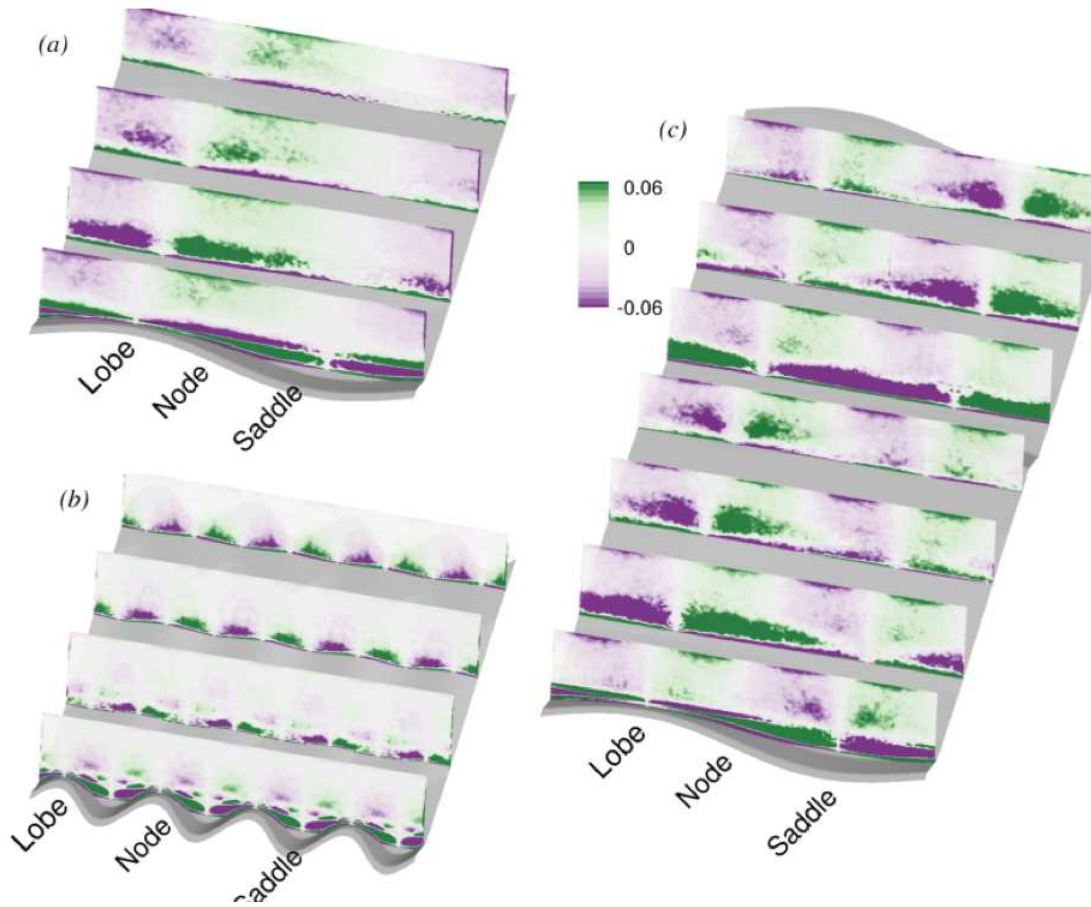


Figure 5. Contours of mean streamwise vorticity, Ω_{xh}/U_b . (a) Case 1, long wavelength; (b) Case 9, short wavelength; (c) Case 10, long wavelength, staggered crests.